

REBOUND: Defending Distributed Systems Against Attacks with Bounded-Time Recovery

Neeraj Gandhi

University of Pennsylvania

Edo Roth

University of Pennsylvania

Brian Sandler

University of Pennsylvania

Andreas Haeberlen

University of Pennsylvania

Linh Thi Xuan Phan

University of Pennsylvania

Abstract

This paper shows how to use *bounded-time recovery* (BTR) to defend distributed systems against non-crash faults and attacks. Unlike many existing fault-tolerance techniques, BTR does *not* attempt to completely mask all symptoms of a fault; instead, it ensures that the system returns to the correct behavior within a bounded amount of time. This weaker guarantee is sufficient, e.g., for many cyber-physical systems, where physical properties – such as inertia and thermal capacity – prevent quick state changes and thus limit the damage that can result from a brief period of undefined behavior.

We present an algorithm called REBOUND that can provide BTR for the Byzantine fault model. REBOUND works by detecting faults and then reconfiguring the system to exclude the faulty nodes. This supports very fine-grained responses to faults: for instance, the system can move or replace existing tasks, or drop less critical tasks entirely to conserve resources. REBOUND can take useful actions even when a majority of the nodes is compromised, and it requires less redundancy than full fault-tolerance.

ACM Reference Format:

Neeraj Gandhi, Edo Roth, Brian Sandler, Andreas Haeberlen, and Linh Thi Xuan Phan. 2021. REBOUND: Defending Distributed Systems Against Attacks with Bounded-Time Recovery. In *Sixteenth European Conference on Computer Systems (EuroSys '21), April 26–28, 2021, Online, United Kingdom*. ACM, Edinburgh, Scotland, UK, 17 pages. <https://doi.org/10.1145/3447786.3456257>

1 Introduction

Defending distributed systems against Byzantine faults is a well-studied problem, and many solutions are already available, such as PBFT [25] or Zyzzyva [74]. However, most of the existing solutions have two things in common: 1) they assume an *asynchronous* system, in which very little is known about the time it takes to transmit messages or perform computations, and 2) they aim for full fault *tolerance* – that is, they attempt to mask all symptoms of a fault, so that the system can continue operating as if all nodes were correct.

There are many use cases where these two assumptions are good choices. However, they come at a price: there are hard theoretical limits on what can be achieved in this setting – including, for instance, the FLP impossibility result [46] and the known lower bound of $3f + 1$ replicas for asynchronous

BFT [19, 78], which tends to cause a considerable overhead. Perhaps more importantly, the resulting guarantees do not make any reference to time: for instance, the liveness guarantee tends to promise only that something will happen “eventually”. In an asynchronous system, this is inevitable – there is simply no way to provide a hard time bound.

However, we observe that there are (also) application scenarios where these assumptions are neither necessary nor sufficient. A prime example is *cyber-physical systems* (CPS), such as an industrial control system or the on-board control network of a car. These systems are bona fide distributed systems – a modern car can have hundreds of components – and attacks on them are quite common [30, 48, 49, 75, 80, 81, 99, 119]. However, out of necessity, they 1) have been carefully engineered for precise timing – with tight bounds on message delays, careful network arbitration, and bounds on the worst-case execution time of pretty much every single computation – and they 2) tend to rely on embedded processors and thus tend to be heavily resource-constrained. Because of this, asynchronous BFT protocols are not necessarily an efficient choice: they work hard to tolerate asynchrony, which CPS do not need, and they spend considerable resources on doing so, which most CPS cannot afford.

One way to lower the cost while preserving full fault tolerance would be to use a synchronous BFT protocol, such as [2]; in this case, the lower bounds are somewhat better ($2f + 1$ replicas). However, cyber-physical systems *also* do not always need to completely mask all symptoms of a fault or attack, because the physical part usually has some inertia that limits damage at very small time scales. For instance, suppose the attacker gains control over a burner that is under a vat containing a volatile compound. The attacker can run the burner continuously and eventually cause an explosion, but lasting damage would occur only after several seconds or minutes, not instantly. Because of this, the system can tolerate (very) short periods in which the control system behaves arbitrarily, *as long as the system returns to the correct behavior within a short amount of time*. The precise amount of time depends heavily on the specific system – we have found values ranging from 500 ms for building control [93] all the way down to 20 μ s for DC/DC converters [52]. Not all of these values may be long enough for a practical defense, but there are definitely some where a solution seems plausible.

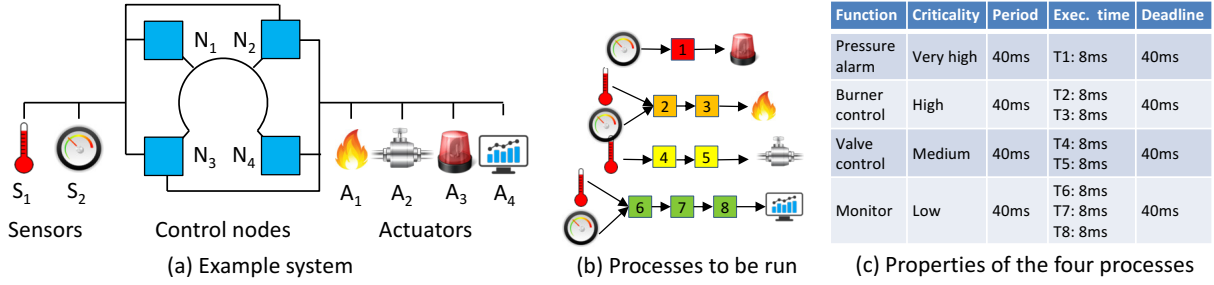


Figure 1. Example scenario with two sensors, four control nodes, and four actuators.

Recently, we proposed *bounded-time recovery* (BTR) [31] as a new approach to fault tolerance in this setting. BTR embraces the time bounds that CPS (and, increasingly, other systems, such as data centers [68]) can provide, and it gives up on the goal of masking all symptoms of a fault. Instead, the system can go through a brief period of arbitrary behavior when a fault occurs, but it is guaranteed to return to the correct behavior within a bounded amount of time.

Our initial BTR protocol, Cascade [50], tolerates only crash faults. This leaves the question whether BTR can work in an adversarial environment. The answer is not obvious, because the presence of an adversary makes the problem considerably more challenging: for instance, BTR requires a way to quickly detect faults, which an adversary can try to prevent, and it requires a short time bound on recovery, which an adversary can try to delay or disrupt. To truly achieve BTR, the system would need to (provably) recover from faults within bounded time, *no matter what the adversary does*.

In this paper, we show that BTR can indeed be extended to the Byzantine model, and we present a BTR algorithm called REBOUND that is suitable for this model. REBOUND operates the system in different *modes*; each mode is intended for a particular failure pattern and specifies a particular mapping of tasks to nodes. (Example: “If node X is faulty, run tasks A and B on node Y and task C on node Z.”) The modes can be computed automatically, based on the workload, or the system designer can make her own choices. At runtime, REBOUND detects faults and creates evidence of detected faults, which is distributed to the entire system; each node independently verifies the evidence, updates its local knowledge of the current failure pattern, and then performs a *mode transition* to the appropriate new mode.

REBOUND offers some properties that are quite different from those of classical fault-tolerance algorithms. Since it does not require consensus, the classical impossibility results and lower bounds do not apply; thus, $f + 1$ replicas are sufficient to handle up to f Byzantine faults, and it is possible for a system to take at least some useful actions even when it is partitioned or more than half of its nodes fail. BTR also supports fine-grained actions in response to faults; for instance, it can reassign tasks to different nodes, replace them with other tasks, or drop less critical tasks entirely (e.g., when

there are no longer enough nodes to run all tasks). This offers interesting new possibilities for system designers.

We have implemented REBOUND, and we have evaluated it using simulations, a small hardware testbed, and an automotive case study. Our evaluation shows that REBOUND is effective, scales well, and has a reasonable overhead.

2 Overview

We begin with a quick overview of the problem, and of the approach we use to solve it.

2.1 Is BTR just for cyber-physical systems?

Although we present our solution in the context of CPS, REBOUND is in fact a general technique that should be broadly applicable in any setting where 1) there is a need to tolerate non-crash faults, 2) timeliness is important, 3) some amount of synchrony is available, and 4) occasional, short periods of incorrect outputs can be tolerated. One non-CPS example of such a setting is video streaming, where delays and data corruption can lead to visible artifacts and should be avoided whenever possible, but where a brief glitch of perhaps a few hundred milliseconds seems harmless – especially if it happens only during an attack or a major equipment failure. Another example setting is stream processing: in many real-world data streams, such as stock market feeds, corrections or updates of previously processed data can occur naturally and are made available via revision records, which can then be used to quickly update the processed data [12].

However, as discussed earlier, cyber-physical systems are a particularly good fit for REBOUND. Since some readers may not be familiar with this type of system, we provide a very brief overview next. For more details, please see [31].

2.2 What are cyber-physical systems like?

At a high level, a cyber-physical system (CPS) is simply a distributed system that interacts directly with the physical world, through sensors and actuators; we sketch a simple example in Figure 1(a). For instance, factory control systems [91], avionic systems [35], building control systems [32], robots [111], and self-driving vehicles [9] are all instances of CPS. Modern CPS can be quite large: for instance, a typical

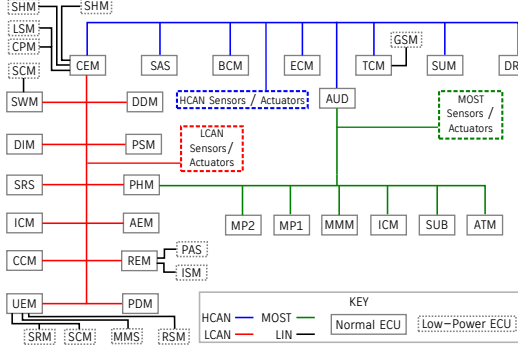


Figure 2. Volvo XC90 on-board network, based on [92].

car contains about a hundred microprocessors [29], as well as many different sensors and actuators.

However, there are also some major differences between CPS and classical data-center systems. For the purposes of this paper, the following differences are important:

Timing is critical: To ensure safety, many CPS must respond quickly to changes in the environment. For instance, when a factory control system senses a pressure increase, it may need to open a safety valve. A delayed response can cause physical damage and/or loss of life. Because of this, CPS must be able to *guarantee* bounds on their response times. This is a major difference to data-center systems, where it is often enough to ensure that *most* responses are fast.

Synchrony is available: In an asynchronous system, it is simply impossible to provide timing guarantees. Therefore, CPS are typically built to be synchronous: software is carefully designed and analyzed to provide worst-case execution times (WCETs), and networks offer predictable timing by explicitly scheduling transmissions to prevent queueing delays and queue drops. Packets can still be lost occasionally due to transmission errors, but the network hardware is designed to avoid this (e.g., by using cables with heavier shielding), and errors can be further reduced with techniques such as forward error correction. To prevent the timing properties from being lost when nodes fail, networks often contain special hardware mechanisms, such as a bus guardian [108, 110], to prevent individual nodes from gaining more than a certain share of the bandwidth.

Occasional errors can be okay: Many CPS inputs (especially from sensors) are inherently noisy; hence, CPS software is typically designed to tolerate brief mistakes or omissions in the input, even in the absence of attacks. Control algorithms can be designed to preserve stability under these conditions [97, 106, 125]. Similarly, actuators are typically connected to physical systems that cannot change their state very quickly; thus, brief glitches in the system’s outputs can be acceptable, as long as the system recovers quickly enough. The meaning of “quickly enough” depends on the system; we show some examples for different systems in Table 1.

| | |
|------------------------------------------|------------|
| DC/DC converters (STM) [52] | 20 μ s |
| Direct torque control (ABB) [53, 95] | 25 μ s |
| AC/DC converters [100] | 50 μ s |
| Electronic throttle control (Ford) [115] | 5ms |
| Traction control (Ford) [18] | 20ms |
| Micro-scale race cars [24] | 40ms |
| Autonomous vehicle steering [15] | 50ms |
| Energy-efficient building control [93] | 500ms |

Table 1. Timescales for recovery (from [90]).

Networks are not fully connected: In data-center systems, it is common to simply assume that the network provides all-to-all connectivity, even when some nodes are compromised. In contrast, CPS networks often have complex topologies that consist of a mix of several buses and point-to-point links; Figure 2 shows, as an example, the on-board network of a modern car. Because of this, some pairs of nodes can only communicate by relaying messages through other nodes, and an adversary may be able to partition the system by compromising certain sets of nodes. However, these complex topologies also offer interesting opportunities [101]: for instance, buses provide limited broadcast channels that can help to prevent equivocation. We exploit some of these opportunities in Section 3.5.

Resources are often scarce: CPS are often deployed in scenarios where there are limits on the available power, space, cost, weight, or a combination of these. Because of this, CPUs tend to be far less powerful than the CPUs in workstations or servers – in fact, a system will often contain the least powerful CPU that is fast enough to do the job. Thus, the fewer resources a fault-tolerance solution needs, the higher its chances of being deployed. (Fortunately, this does not mean that cryptography is out of the question: CPUs often contain accelerator hardware for cryptographic operations, or accelerators can be added as external coprocessors.) CPUs and networks vary, but it is fairly common to find ARM cores or comparable CPUs, and network speeds between 5 Mbps (CAN bus) and 1 Gbps (Industrial Ethernet).

As discussed earlier, these properties are a particularly good fit for REBOUND: CPS have the synchrony that REBOUND needs, they need the timing guarantees that REBOUND provides, and they can benefit from REBOUND’s lower overhead. Also, many CPS can tolerate short bursts of incorrect output, in which case the BTR property is a plausible alternative to “perfect” fault tolerance.

2.3 System model and workload

We assume a system with three kinds of nodes: *sensors*, which periodically provide inputs from the outside world, *actuators*, which send outputs to the outside world, and some set N of *controllers*, which perform computations. The nodes can communicate using a network that is highly reliable but not necessarily fully connected – it can consist of a mix of buses and point-to-point links. The capacity of each link is known,

and we assume that, as discussed above, there is a hardware mechanism that prevents faulty nodes from gaining more than their share of the bandwidth. Each node has a local clock, and clocks are synchronized to within a small time difference.

We assume a workload that consists of data flows, each originating at some of the sensors, crossing some controllers, and terminating at some of the actuators. This is a common model for CPS [126]. We illustrate this model using our simple example from Figure 1(a), which is an industrial control system from a chemical plant. This system has four data flows, which control a burner, a valve, a monitor, and a pressure alarm, based on inputs from a pressure gauge and a temperature sensor. The sensors and actuators are attached to a chemical reactor. Each flow can contain several tasks; here, the flows have between one and three, which are shown as numbered squares in Figure 1(b). Flows can be *active* or *inactive*; each task of an active flow must be executed periodically on one of the controllers. We assume that the tasks are deterministic and that their period, worst-case execution time, and deadline of each task are known. Figure 1(c) shows some concrete values for our example. We also assume that, as is common in CPS [21], each flow has been assigned a *criticality level* [116], so the system can triage the flows when it no longer has enough resources to run all of them.

2.4 Definitions and goals

We say that a controller is *correct* as long as its externally observable behavior is consistent with the tasks it has been assigned – that is, as long as it is producing the right outputs at the right time, given the inputs it has received so far. Once a controller is no longer correct (perhaps because it has changed, delayed, or omitted an output, or produced an extra output), we say that it is *faulty*, and we continue to consider it faulty until it is repaired and “blessed” by an external operator. We say that the controller *fails* at the moment where it transitions from correct to faulty; of course, something could have gone wrong inside the node before that moment, but if so, it has not yet affected its externally observable behavior.

Our definition of a fault is consistent with the Byzantine model [78], except that we also consider attacks on timing. This is important for CPS: for instance, a faulty controller could cause an explosion simply by delaying a (valid) command to shut off the burner. Note that we consider only attacks on the controllers and not, say, an attacker who puts an ice pack on a temperature sensor; there are orthogonal solutions, such as attack-resilient state estimation [94], that deal with sensors and actuators.

We have two simple goals. The first is that all active data flows are executed on correct nodes, except for very brief periods after a node fails. In other words, if no node fails during interval $[t - R_{\max}, t]$, then all active data flows should be running on correct nodes at time t . We call R_{\max} the *maximum recovery time*; recall that this is a worst-case bound, and that it depends on the system (see Table 1). Our second goal

is that the system should keep as many data flows active as it can, though it may deactivate the least critical flows when it no longer has enough resources to execute them all.

2.5 Threat model

We assume an adversary who is able to cause up to $f_{\max} < |N|$ of the compute nodes or links to fail, but no more than f_{conc} of them “concurrently” – that is, within the same interval of length R_{\max} . It is fine to set $f_{\text{conc}} = f_{\max}$; we decided to separate the two parameters because some costs depend only on f_{conc} . For instance, $f_{\text{conc}} < f_{\max}$ could be used for less powerful adversaries who are not able to synchronize faults to within a few milliseconds, or for tolerating a combination of adversarial and non-adversarial faults. Notice that each new fault restarts the R_{\max} clock; if there is an end-to-end bound R on the time the system can spend recovering, it would be necessary to set $R_{\max} := \frac{R}{f_{\text{conc}}}$.

As usual in the fault-tolerance literature, we do not consider $f_{\max} = |N|$: if the adversary can compromise every single node in the system, there is very little that can be done. Physical security can prevent the adversary from tampering with too many nodes, and software and hardware heterogeneity, which already exists in many CPS, can help to prevent correlated faults, e.g., due to shared vulnerabilities. However, we *do not* put any other restrictions on possible values for f_{\max} ; it is possible to choose $f_{\max} = |N| - 1$ (although this would be expensive). This is a major difference to BFT, and, at first glance, it seems to contradict the known impossibility results for consensus [46]. But these do not apply here because consensus requires all decisions to be final and correct, whereas BTR allows nodes to sometimes output incorrect values and is thus a different, and slightly “easier”, problem.

2.6 Approach: Modes and mode changes

Our approach is to enable the system to operate in multiple *modes*, which can differ in how they map tasks to nodes. At least conceptually, there is a mode for every possible failure scenario (KN, KL) , where KN and KL represent the sets of nodes and links that are known to have failed. For instance, the mode (\emptyset, \emptyset) is used when all nodes and links are operating correctly, the mode $(\{N_1\}, \emptyset)$ is used when node N_1 fails, etc. Then, at runtime, we run a protocol that detects when faulty nodes start to deviate from their expected behavior (at a high level, by running a few replicas and comparing their outputs), and, whenever a new fault is detected on a node or a link, we use the recovery period to perform a *mode change* to the appropriate new mode. This will involve a brief period of “chaos”, as nodes transition from one mode to another, but, as long as the transition is complete before the recovery period ends, we can still maintain the BTR guarantee.

As an illustration, Figure 3 shows a few possible modes and mode transitions for the system in Figure 1, with $f_{\text{conc}} = 1$ and $f_{\max} = 3$. The mode on the left is used when all nodes

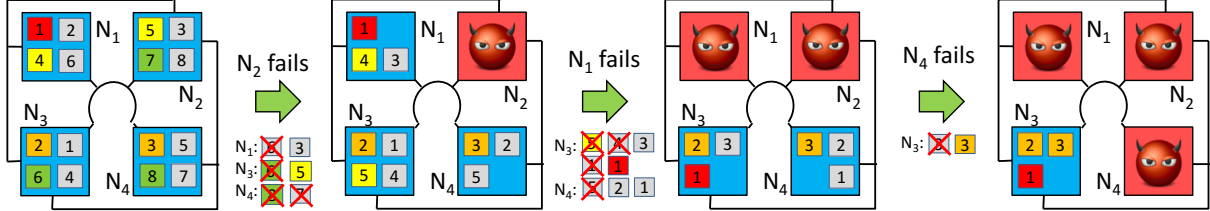


Figure 3. A few mode transitions for the system from Figure 1, with $f_{\text{conc}} = 1$ and $f_{\text{max}} = 3$. The figure shows which of the tasks from are scheduled on which node; task copies are shown in gray. Each node can run up to four tasks or task copies.

and links are operating normally; notice that each task has one replica, which is shown in gray. When N_2 fails, the system responds by moving task τ_5 to N_3 and by reconfiguring some of the replicas; additionally, since the system no longer has enough nodes to run the entire workload, the least critical data flow (monitoring, shown in green) is dropped. If a second node (N_1) fails later, τ_1 is moved, and the valve control task is also dropped, but the two most critical data flows still survive.

2.7 Requirements

Next, we state the four properties we need to make this approach work. (In an extended version of this paper [51, §A], we formally prove that REBOUND has these properties.)

Requirement 1 (Completeness). *For each observable fault, at least one faulty node or link is detected by at least one correct node.*

By “observable fault”, we mean a fault that directly or indirectly affects at least one correct node. This restriction is necessary to rule out faults that have no visible effects at all, such as an unused bit flipping in a node’s memory, or two faulty nodes whispering evil messages over a direct link between them but otherwise acting correctly. Please see [60] for a formal definition.

Next, we add a notion of time; “eventual” detection is not enough because, in our scenario, the adversary can win simply by delaying the detection process long enough, e.g., by distracting the other nodes with enormous garbage messages. Thus, we add the following requirement:

Requirement 2 (Bounded-time detection). *If an observable fault occurs at time t , it must be detected by time $t + T_{\text{det,max}}$.*

Once a node has detected a fault, it must trigger a mode transition. However, most faults are not directly visible to all nodes – for instance, a malicious message would only be directly visible to the node that receives it. If we allowed nodes to simply report faults to other nodes without further evidence, a compromised node could abuse this mechanism to report fabricated faults, or to sow confusion by triggering transitions to random modes. To avoid this, we add the following:

Requirement 3 (Accuracy). *If a node or link is not faulty, no correct node will consider it to be faulty.*

We accomplish this by having the node that first detects the fault generate *evidence* of the fault, by distributing any such

evidence across the system, and by requiring nodes to verify the evidence before they “believe” a new report of a fault that they did not directly observe. The verification can be done independently by each node and does not require consensus.

How should the system transition to a new mode? The natural approach would be to appoint a single coordinator node, or a group of nodes that agree on which mode to use. However, it is critical that we avoid both: the former because it would create a single point of failure, and the latter because of the known impossibility results [19, 46, 78]. Fortunately, in our case, it is sufficient to simply flood the evidence through the system: each node can verify it independently and then *locally* transition to the new mode, without coordinating with other nodes. The correct nodes will collectively transition to the same mode – albeit in an unsynchronized, somewhat messy way – *as long as* we can ensure that they all receive the same evidence within a sufficiently short amount of time.

This last point creates a final complication: since we did not assume all-to-all connectivity, we must consider the possibility that the faulty nodes can partition the network or selectively refuse to forward certain messages to certain nodes. Thus, we cannot hope to achieve global consistency, much less within bounded time. However, a slightly weaker property is sufficient for our purposes:

Requirement 4 (Bounded-time stabilization). *If a correct node i has valid evidence e , then, within bounded time $T_{\text{stab,max}}$, each correct node j will either 1) receive e , or 2) conclude that i is unreachable.*

Thus, if the adversary does manage to partition the system, each partition will at least be aware of its own extent, and can make local decisions independently. During a partition, it will not always be possible to mask all the symptoms of the fault – for instance, if the sensors and actuators for some data flows end up in different partitions, such flows can obviously not continue. However, a system can take other actions in response, such as scheduling new or different tasks in the partitions. For instance, in Figure 1, a partition that contains the burner but not the temperature sensor could schedule a new task that shuts off the burner, and a partition that contains the warning light but not the pressure gauge could schedule a task that activates the light to get the operator’s attention.

Collectively, the four requirements are sufficient for BTR: If it can take a node up to $T_{\text{switch,max}}$ to switch to another mode, and $T_{\text{det,max}} + T_{\text{stab,max}} + T_{\text{switch,max}} < R_{\text{max}}$, each observable fault will, within bounded time R_{max} , cause all correct nodes to transition to a new mode, and the mode will be consistent among the correct nodes in each partition.

3 The REBOUND algorithm

We now present REBOUND, an algorithm that meets these four requirements. REBOUND relies on standard cryptographic assumptions: it assumes that each node i has a public/private keypair (π_i, σ_i) , that each node knows the public key of all other nodes, and that there is a cryptographic hash function H . REBOUND proceeds in discrete, numbered *rounds*, which could, e.g., be the periods of the underlying workload. REBOUND guarantees a bound on the number of rounds it can take to detect a fault; thus, shorter rounds result in a lower detection bound $T_{\text{det,max}}$.

3.1 Roadmap

Existing fault-tolerance protocols typically assume that the network is fully connected and that, at least logically, any pair of nodes can always communicate. For REBOUND, we want to avoid this assumption: many CPS use a mix of different buses and links, and messages can often reach their destination only if they are forwarded by some of the nodes, which a faulty node may not always do.

To avoid a circular dependency between fault detection and communication, REBOUND consists of two layers: a *forwarding layer* and an *auditing layer*. The forwarding layer (Section 3.3–3.4), has the following four functions. 1) It accepts, for each mode m , a set of data paths $\text{PATH}(m)$ between nodes that should exist in that mode. In each round, it picks up a data packet at the source of each path and transports it to the corresponding sink. 2) It accepts and further distributes evidence to all correct nodes in the sender’s partition. 3) It detects when nodes fail to perform the first two functions correctly, and generates evidence of such faults, which it also distributes. And 4) it selects the local mode on the node it is running on based on the available evidence. We also describe a number of optimizations (Section 3.5–3.6) that substantially reduce the cost of the forwarding-layer algorithm.

The auditing layer (Section 3.7–3.8) accepts 1) a set of data flows, and 2) a schedule for each mode m (Section 3.9) that maps the tasks in each flow, as well as f_{conc} copies of each task, to specific nodes. Using the data flows and schedules, the auditing layer gives two kinds of paths to the forwarding layer: a) paths that connect tasks to their upstream and downstream neighbors; and b) “internal” paths that connect tasks to their copies and are used for application-level fault detection. The data flows, schedules, and path representations are computed offline. At runtime, the auditing layer is responsible for verifying that, given a set of inputs at a particular

time and previous state, the produced output is correct. If verification fails, this is evidence of a fault that is passed to the forwarding layer for distribution.

3.2 Generating evidence

There are two ways a node can fail: it can either send a bad message (commission fault) or fail to send, at the correct time, a good message it was expected to send (omission fault). Since we need all the nodes to make a mode transition in response to a given failure, but each commission or omission will be visible to only some of the nodes, we cannot avoid having the nodes exchange information about what they each have seen. However, faulty nodes can tell lies, and since we need accuracy, a correct node A must never simply “believe” another node B that a third node C has said or done anything – it must always have some concrete evidence.

Since messages are signed, evidence of commission faults is easy: if a controller produces a bad output, that output and the corresponding inputs constitute a *proof of misbehavior (PoM)*, which can be verified by other nodes and can thus serve as evidence. But what about omission faults? Since we consider a synchronous environment, a node can always tell when it should expect a message to arrive.¹ But in general, an omission fault is visible only to the recipient – how would a node prove to others that it has *not* received a given message? Our approach is to simply allow both endpoints to issue a *link failure declaration (LFD)*, which is a message $\sigma_i(\text{LFD}(i, j))$ that says that i and j can no longer properly communicate. A single LFD does not attribute the failure specifically to i or j , but this is also not necessary – since the link is clearly not working, it should no longer be used, and a mode transition may be necessary to redirect its flows.

Notice that we *can* sometimes infer node faults from multiple LFDs. Suppose, for instance, that $f_{\text{max}} = 1$ and a node A issues LFDs for two links (A, B) and (A, C) . This means that both $\{A, B\}$ and $\{A, C\}$ must contain at least one faulty node. But if $f_{\text{max}} = 1$, B and C cannot both be faulty, so the only possible explanation is that A has failed. In general, we can always map a mode (KN, KL) with $|\text{KN}| + |\text{KL}| > f_{\text{max}}$ to another with $|\text{KN}| + |\text{KL}| \leq f_{\text{max}}$, by replacing some link faults with node faults. (If $i \in \text{KL}$, we implicitly consider all of i ’s links to be faulty, and we do not include them in KL .)

3.3 Evidence distribution

As a first approximation, REBOUND’s forwarding layer distributes evidence of node or link faults by flooding it through the entire system: in each round, each node i sends all of its evidence E_i to each of its neighbors, and it verifies and stores any new evidence it receives from them. However, this is not

¹The network itself almost never loses packets. Everything is scheduled, so there is no loss due to congestion, which leaves only link-layer loss. In our testbed, we were able to send 10^9 packets without seeing a single loss.

```

1: var  $\text{HBT}_i = \emptyset$  ▷ Heartbeats remembered by node  $i$ 
2: var  $\text{MSG}_i = \emptyset$  ▷ Messages seen by node  $i$ 
3: var  $\text{POM}_i = \emptyset$  ▷ Proofs of misbehavior seen by node  $i$ 
4:
5: /* Invoked if node  $i$  receives a message  $m$  from node  $j$  in round  $r */
6: function RECEIVE( $i, j, r, H, M$ )
7:   if  $\text{!IS-PLAUSIBLE}(H, M)$  then return
8:   if  $M = \text{COMPUTE-MESSAGES}(j, i, r-1, H, \text{MSG}_i \cup M)$  then
9:      $\text{HBT}_i = \text{HBT}_i \cup H$ 
10:     $\text{MSG}_i = \text{MSG}_i \cup M$ 
11:   for each  $\sigma_n(n, r, E) \in H : \text{HBT}_i.\text{CONTAINSHEARTBEAT}(n, r)$  do
12:      $h = \text{HBT}_i.\text{GETHEARTBEAT}(n, r)$ 
13:     if  $\sigma_n(n, r, E) \neq h$  then
14:        $\text{POM}_i = \text{POM}_i \cup \sigma_i(\text{POM}(n, \sigma_n(n, r, E), h))$ 
15: /* Invoked after node  $i$  has received all messages in round  $r */
16: function FINISH-ROUND( $i, r$ )
17:    $H_{\text{new}} = \text{COMPUTE-HEARTBEAT}(i, r, \text{HBT}_i, \text{MSG}_i, \emptyset)$ 
18:    $\text{HBT}_i = \text{HBT}_i \cup \sigma_i(H_{\text{new}})$ 
19:   for  $p \in \text{PATH}(\text{HBT}_i, \text{EVIDENCE})$ :  $p = (i, \dots)$  do
20:      $\text{MSG}_i = \text{MSG}_i \cup \{\text{GENERATE-MESSAGE}(p, r)\}$ 
21:   for  $k \in \text{NODES}$ :  $(i, k) \in \text{EDGES}$  do
22:      $M = \text{COMPUTE-MESSAGES}(i, k, r, \text{HBT}_i, \text{MSG}_i)$ 
23:     if  $\{\text{LFD}(i, k), \text{POM}(k)\} \cap \text{HBT}_i.\text{EVIDENCE} = \emptyset$  then
24:        $\text{SEND}(k, (\text{HBT}_i, M))$$$ 
```

```

25: function COMPUTE-HEARTBEAT( $n, r, H, E_{\text{new}}$ )
26:   if  $((r > 0) \wedge \text{!}H.\text{CONTAINSHEARTBEAT}(n, r-1))$  then return  $\perp$ 
27:    $E = (r == 0) ? \emptyset : H.\text{GETHEARTBEAT}(n, r-1).\text{EVIDENCE}$ 
28:    $E = E \cup E_{\text{new}}$ 
29:   for  $(k : (k, n) \in \text{EDGES} \wedge \text{LFD}(k, n) \notin E)$  do
30:     if  $H.\text{CONTAINSHEARTBEAT}(k, r-1)$  then
31:        $h = H.\text{GETHEARTBEAT}(k, r-1)$ 
32:        $E_{\text{new}, k} = \{\text{LFD}(x, y) \in h \mid x = k \vee y = k\}$ 
33:        $h' = \text{COMPUTE-HEARTBEAT}(k, r-1, H, E_{\text{new}, k})$ 
34:       if  $(h = h')$  then  $E = E \cup h.\text{EVIDENCE}$ 
35:       else  $E = E \cup \{\text{LFD}(k, n)\}$ 
36:     else  $E = E \cup \{\text{LFD}(k, n)\}$ 
37:   return  $(n, r, E)$ 
38: function COMPUTE-MESSAGES( $n_{\text{from}}, n_{\text{to}}, r, H, M$ )
39:    $E = H.\text{GETHEARTBEAT}(n_{\text{from}}, r).\text{EVIDENCE}$ 
40:    $M' = \emptyset$ 
41:   for  $(k : (k, n_{\text{from}}) \in \text{EDGES} \wedge \text{LFD}(k, n_{\text{from}}) \notin E)$  do
42:      $M' = M' \cup \text{COMPUTE-MESSAGES}(k, n_{\text{from}}, r-1, H, M)$ 
43:    $M' = \{m \in M' \mid m.\text{PATH} \in \text{PATH}(E) \wedge (n_{\text{from}}, n_{\text{to}}) \in m.\text{PATH}\}$ 
44:   for  $p \in \text{PATH}(E)$ :  $p = (n_{\text{from}}, \dots)$  do
45:     if  $\text{!}M.\text{CONTAINSMESSAGE}(p, r)$  then return  $\perp$ 
46:     else  $M' = M' \cup M.\text{FINDMESSAGE}(p, r)$ 
47:   return  $M'$ 

```

Figure 4. Pseudocode for REBOUND’s forwarding layer, without the optimizations from Sections 3.5–3.6.

enough, since a malicious node could refuse to forward information from correct nodes. To get bounded-time stabilization, we must guarantee that, whenever a correct node has new evidence, all other correct nodes will receive that evidence within bounded time, unless they have been partitioned off.

At first glance, it may seem that we can achieve this by having each node i flood a signed *heartbeat* $\sigma_i(r, E_i)$ instead of merely E_i , and by having any other node j insist that it receive such a message from i in round $r+k$, where k is the length of the shortest path from i to j . However, it is not that simple: if j does not receive i ’s heartbeat, then j can conclude that this is i ’s fault *only* if i and j are directly connected – if they are not, any other node along the path could have dropped the message as well. Hence, we need a way to attribute message drops to a particular node or link.

We achieve attribution by, in effect, insisting that each node along the path include *either* the message itself *or* some evidence that explains why the message is missing. Suppose, for instance, that the path is $i \rightarrow x \rightarrow y \rightarrow j$. Then, in round r , j can expect to receive from y either $\sigma_i(r-3, E_i)$ or evidence that either a) $i \rightarrow x$ failed in round $r-2$ or earlier, b) $x \rightarrow y$ was faulty in round $r-1$ or earlier, or c) x or y were faulty in rounds $r-2$ or $r-1$, respectively. If y is correct, it can always provide one of these things by making a similar demand of x in the previous round – and, if y does not receive a suitable explanation from x , y can generate one simply by declaring the link $x \rightarrow y$ to be faulty.

3.4 Basic forwarding layer

Figure 4 shows the pseudocode for REBOUND’s forwarding layer. Each node i maintains sets HBT_i and MSG_i of the heartbeats and messages it has received so far. In each round, nodes expect to receive a message with new heartbeats and messages from each of their neighbors, and, when such a message arrives, they simply merge this information with their local sets (lines 6–10). If a node is found to have signed two conflicting heartbeats for the same round, this constitutes a PoM against that node (lines 11–14). At the end of each round, each node computes a new heartbeat (lines 17+18), generates a new data packet for each path that originates on it (lines 19+20), and then sends these packets, together with any packets the node is simply forwarding, to the relevant neighbor (lines 21–24).

The crux of the algorithm is the COMPUTE-HEARTBEAT function, which computes the heartbeat that a node n *should* send in a round r , assuming that it has seen sets of heartbeats H and has issued a set E_{new} of LFDs since the last round. Since the sets are monotonic, COMPUTE-HEARTBEAT starts with i ’s sets from the previous round (lines 26+27) and then adds in the new LFDs from E_{new} (line 28). This is necessary because LFDs are issued based on local observations, so i cannot, and need not, verify them directly – it simply gives credit to its neighbor’s LFDs. The function then iterates over each of i ’s neighbors; for each neighbor k , it locates the heartbeat h – if any – that k has sent to i in the previous round (line 31) and then calls itself recursively (line 33) to recompute the heartbeat h' . If h exists and $h = h'$, the neighbor’s heartbeats are added to the computed sets (line 34), just as i would actually have done in the RECEIVE function; otherwise, an LFD is

added to the evidence set (lines 35+36). COMPUTE-MESSAGES uses a similar, recursive approach to compute the set of messages that node n_{from} should send to node n_{to} in round r .

In our extended version [51, §A], we provide a formal statement of the properties from Section 2.7, as well as proofs that our algorithm has them. The extended version also describes some additional refinements [51, §B].

3.5 Optimizations

As described so far, the REBOUND is very expensive: in each round, it sends $O(r \cdot |N|)$ messages over each link (one from each past round on every other node), and it separately verifies the signatures on, and the information in, each of these messages. However, we can do a lot better: most of the messages are duplicates, and only the messages for the most recent round per node are actually new. By sending only these messages, and by having each node remember the previous ones, we can reduce the message complexity to $O(|N|)$ per link. This also helps with the computation complexity: the remembered messages have already been checked, so each node only needs to check the $O(|N| \cdot d)$ new messages per round, where d is the degree of the node.

A second refinement reduces the storage complexity. For each pair of nodes i and j , let $D_{i,j}$ be the maximum length of the shortest path from i to j in any topology that can be derived from the original graph by removing up to f_{\max} nodes, without disconnecting i and j . We call $D_{i,j}$ the *max-fail distance* between i and j ; intuitively, it is the maximum number of rounds it can take for information to propagate from i to j under any failure scenario we consider. If j receives $\sigma_i(r, E_i)$ for the first time in a round $r' > r + D_{i,j}$, we know that it must have been delayed somewhere, so we can simply ask all correct nodes to consider such messages to be invalid. With this change, each node i needs to store only the most recent $D_{i,j}$ messages from each other node j .

A third refinement concerns bus-type links. In principle, such links could simply be treated as a collection of point-to-point links among all the nodes on the bus. However, there are two opportunities for optimization: first, since the heartbeats that a correct node sends to its neighbors in a given round are identical, we can simply broadcast the heartbeats on the bus instead of sending individual messages. And second, instead of having *each* node verify the signature on each broadcast heartbeat, we can have each signature be verified by a subset of $f_{\max} + 1$ nodes, which must include at least one correct node. If a node discovers that a signature is incorrect, it can broadcast a challenge to the other nodes, who can then check the relevant signature on their own and conclude that either the sender or the challenger is faulty.

3.6 Multisignatures

Next, we observe that in a stable state, if we exclude the signature and round number, many $\sigma_i(r, E_i)$ messages contain identical evidence sets because all the nodes in a given

partition have the same evidence. Thus, we can avoid the corresponding cost by using multisignatures [67, 85] – e.g., the construction from Boldyreva [17]. With this, messages can be signed by sets of nodes, and signatures from different sets can be combined into a single signature. Since a node might receive evidence in different combinations on different links, we also divide the heartbeats $\sigma_i(r, E_i)$ into two separate messages $\sigma_i(r, |\Delta E_i|)$ and $\sigma_i(r, e_{i,x})$, where $e_{i,x}$ is a *single* piece of evidence and the two “halves” are only accepted if they match.

With these changes, a node i might receive a heartbeat from nodes j and k over one link and an aggregate heartbeat from j, l, m over another; it can then efficiently check each signature (in constant time) and combine them with its own to form a signature from i, j, k, l, m . (Notice that j ’s signature is included twice; this is harmless.) With this change, each node i only needs to send $O(D_{i,\max})$ messages over each of its links (where $D_{i,\max} = \max_j D_{i,j}$) in the common case, and the number of signatures that need to be checked is $O(D_{i,\max})$. The aggregate public keys for the verification can be precomputed based on the current mode: if an update supposedly originated on node Ω in round R_1 , a node i should expect to receive in round R_2 , from a neighbor j , a signature from any node k such that a path of at most $R_2 - R_1$ hops exists from Ω to j that also includes k . In cases where a node needs to be added or removed, the aggregated public keys can be efficiently updated in $O(\log |N|)$ steps using a binary tree.

What about the worst case? Let d be the maximum degree of any node, and suppose $d > f_{\max}$. In general, each of the f_{\max} faulty nodes can send f_{\max} LFDs on each of its d links to a given neighbor without being declared faulty immediately, and it can issue them in different rounds, to complicate aggregation. Thus, in the worst case, $f_{\max}^2 \cdot d$ notifications can all arrive at the same correct node in the same round, causing at most $2f_{\max}^2 \cdot d$ signature checks per round.

3.7 Auditing layer

So far, we have described REBOUND’s forwarding layer, which provides node-to-node data paths but does not check how the nodes process the data. This is the purpose of the auditing layer, which we describe next.

The auditing layer is inspired by PeerReview [61]. It creates f_{conc} replicas of each task, each on a different node; thus, if there are at most f_{conc} concurrent faults, either the primary task or one of its replicas is always correct, because the faults will trigger a mode change that moves the task and/or replaces replicas on faulty nodes. Auditing nodes use deterministic replay to assess whether the correct output was generated: the auditor uses a local copy of the relevant task, replays the inputs to this copy, and checks whether the outputs match the outputs of the primary. If they do not, a fault has been detected, and the faulty node’s tasks and replicas are reassigned to other nodes.

The replicas have two functions: 1) they repeat the primary’s computations, using the same inputs but not necessarily at the same time, and 2) they verify that the primary does not equivocate. Since we have assumed that tasks are deterministic, a replica should always get the same result as the primary; if not, it hands over the (signed) inputs to the forwarding layer as evidence, which distributes it to the other nodes. The process is analogous when a replica learns that the primary has equivocated; in that event, the evidence consists of two signed but conflicting messages.

When a node i receives evidence from a node j about a task on a node k , it verifies the evidence locally and then adds either j (if the evidence is valid) or k (if it is not) to its local set KN, which triggers a mode transition.

3.8 Audit protocol

In comparison to PeerReview (which was designed for asynchronous systems), our protocol is much simpler because omission faults are already handled by the forwarding layer. In other words, the sink of a path can be sure that, in each round, it either receives *some* correctly signed message from the source of that path, or some node on the path is detected as faulty and a mode transition occurs. As in PeerReview, we structure the messages so that the signature is on a small, detachable *authenticator*, which contains a hash of the message. Thus, the authenticator can be sent instead of the message where the contents themselves are not relevant.

Consider a task τ , with upstream tasks $\alpha_1, \dots, \alpha_x$, downstream tasks β_1, \dots, β_y , and replicas $\rho_1, \dots, \rho_{f\text{conc}}$. Then the auditing layer creates four kinds of paths: 1) paths $\alpha_i \rightarrow \tau$, and $\tau \rightarrow \beta_j$, which carry the flow’s data; 2) paths $\tau \rightarrow \rho_i$, which τ uses to forward its inputs to the replicas; 3) paths $\beta_i \rightarrow \rho_j$, which downstream tasks use to forward authenticators from τ ’s outputs to the replicas; and 4) paths $\rho_i \rightarrow \rho_j$, which the replicas use to exchange authenticators from τ ’s inputs and outputs, to detect equivocation. Each replica 1) checks whether the provided inputs were properly signed by the α_i and are for the current round; 2) forwards the authenticators from the inputs to the other replicas; 3) checks whether the received authenticators are consistent with its own inputs; and 4) repeats τ ’s computations on these inputs and checks whether the output is consistent with the authenticators it receives from the β_i . If any of these checks fails, the replica distributes its information as evidence.

3.9 Scheduling

For each mode it can enter at runtime, REBOUND must have a *schedule* that assigns each task to a specific node and a specific activation pattern. This is different from a classical CPS, which typically has only one schedule for the entire system. In both the classical setting and ours, schedules are *static*; this is fairly common in CPS (see, e.g., [16]). The schedules are interdependent, for at least two reasons. One is that, when transitioning from one mode to another, we would

ideally like to change as little as possible; if we reassign lots of tasks to other nodes, the necessary state transfers may take too long and cause REBOUND to exceed the recovery bound. The other reason is that we must prevent the system from scheduling itself into a corner, e.g., by moving many tasks to a part of the system that already has very little bandwidth to the rest, and then not being able to move them back out if an additional link fails. In principle, the schedules could be computed on demand, assuming that the maximum recovery time is long enough; however, since we aim for low recovery times, we instead opt to precompute the schedules at compile time, and to store them on each node.

Our starting point is Cascade [50], which focuses on a different fault model (crash faults) but has a fairly similar scheduling problem. Since the modes are interdependent, we organize them into a tree in which the fault-free mode (\emptyset, \emptyset) is at the root, and in which children differ from their parents by exactly one node or link failure; the leaves are modes in which f_{max} nodes have failed. We then formulate our requirements as constraints – e.g., that each node’s workload is schedulable under Earliest-Deadline First (EDF), or that no node has more than one replica of the same task – and we then use an integer linear program (ILP) solver to find suitable schedules bottom-up, with each mode trying to minimize the transition costs to its child modes.

Our scenario differs from Cascade’s in several ways. A few are relatively simple to address: for instance, REBOUND generates and verifies cryptographic signatures when messages are exchanged, its forwarding layer is much more complex than Cascade’s fault detector, and REBOUND’s replicas check their outputs for consistency with the primary’s authenticators, whereas Cascade’s backups just discard their outputs. We can fold the additional costs for these operations into the worst-case execution times (WCETs) of the relevant tasks. Other differences require more substantial changes: for instance, REBOUND supports data flows that are DAGs, whereas Cascade supports only chains, and REBOUND forwards authenticators from the recipient of a message to the sender’s replicas, and also between replicas. We addressed these by changing one of Cascade’s four constraints, and by adding three new ones. We omit the details due to lack of space, but they are available in [51, §C].

4 Implementation

We built a Linux-based prototype of REBOUND. Our prototype can be used for simulations (to explore the parameter space under controlled conditions) but can also directly run on Linux in our testbed (Section 4.1).

Multisignatures: We use the multisignature scheme from Boldyreva et al. [17], which relies on an elliptic curve defined over a Gap Diffie-Hellman group. We implemented this scheme using the PBC Library [13] to perform group operations and to work with pairings.

Key rotation: In REBOUND, signatures need to be secure for only a short time, since messages expire very quickly (after $D_{i,\max}$ rounds). We can exploit this by assigning each node a strong “permanent” keypair (perhaps a 2,048-bit RSA keypair) and by having each node periodically (say, once every hour) generate weaker keys, which it can sign with the strong private key and distribute to the other nodes. Once new keys are received from a node, all old keys become invalid. Thus, for a successful attack, the adversary would need to break the weak keys faster than the nodes generate them.

Parameters: In our prototype, we use 512-bit RSA keys for ordinary signatures. This yields fast operations, but factoring a 512-bit number would still take the adversary several hours [113], which is far longer than the speed at which we rotate them. For the multisignatures, we use a 256-bit group with 160-bit secret keys, which results in similar security. Signatures take 1.17ms to generate and 1.18ms to verify; combining signatures takes $3.34\mu\text{s}$, and combining public keys takes $3.28\mu\text{s}$. For more details on our parameters, please see the extended version [51, §D].

Scheduling: When generating the mode trees, we parallelize the computation per fault layer; for instance, all modes that are reached through a single fault can be computed in parallel with one another, since they do not affect each other. We also use an optimization from Cascade that partitions the system and finds mode trees for the partitions first and then merges them into a mode tree for the entire system. At runtime, nodes use standard EDF for local scheduling. We use Gurobi [57] as our ILP solver.

Protocol variants: We implemented two versions of REBOUND: one with the optimizations from Section 3.5 but not the multisignatures (REBOUND-BASIC) and another with multisignatures enabled (REBOUND-MULTI).

4.1 Testbed

To get a sense of how well REBOUND works on a real embedded platform, we built a small testbed that mirrors the topology from Figure 1(a) with 10 Raspberry Pi 4 boards. Each board has a quad-core ARM Cortex-A72 processor, one GbE port, four USB ports, and 4 GB of RAM; we added 32 GB microSD cards and, for the nodes that had more than one network connection, USB adapters with extra GbE ports. We replaced the buses with standard GbE switches; this seemed like a reasonable approximation of Industrial Ethernet. We installed Raspbian Buster on each node, which comes with a Linux 4.19 kernel.

The workload consisted of the four data flows (eight tasks) shown in Figure 1(b), with the periods, WCETs, and criticality levels from Figure 1(c), plus an additional task for the REBOUND algorithm and one replica for each of the eight tasks – that is, we assume that faults happen one by one ($f_{\text{conc}} = 1$). We configured REBOUND with 40ms rounds, equal to the period of the tasks. Since the topology is small, we use standard

RSA-512 signatures, which take about $750\mu\text{s}$ to generate on this platform, and about $49\mu\text{s}$ to verify. The actuator nodes (A_1 – A_4 in Figure 1) each send their outputs to a GPIO pin using pulse-width modulation (PWM); we use an oscilloscope (Siglent SDS1204X-E) to measure these signals.

5 Evaluation

The goal of our experimental evaluation was to answer three questions: 1) What are the costs of REBOUND?, 2) Is it effective at limiting damage in realistic cyber-physical systems?, and 3) Does it work well on a real embedded platform? We answer the first question with simulations, so we can cover a large part of the parameter space; we answer the second with a simulated case study from automotive systems; and we answer the third using our Raspberry Pi testbed.

5.1 Simulation setup

For our simulations, we generated synthetic workloads and network topologies, so we can explore the parameter space. For the network topologies, we used the Erdős-Rényi $G(n, p)$ model with $p = 3\frac{\ln n}{n}$, a choice that ensures that the networks are connected and have a diameter that grows with $O(\log n)$. We generated networks with $n = 4 \dots 100$ nodes (the most complex of the car models examined in [92] had 65 electronic control units, or ECUs), and we used 10 topologies for each size. For Section 5.4, we generated random workloads with periods in the range [30 ms, 70 ms], application CPU utilization in the range [0.4, 0.7], and task utilization consuming between 25%–100% of the application utilization. The execution time was determined by multiplying a selected task utilization with its period. We set deadlines equal to the period (since the application as a whole is periodic, it can operate only as fast as the period of its slowest task). This is a standard approach for evaluating real-time scheduling techniques; see, e.g., [122]. We generated a set of applications as chains and randomly selected the number of tasks per chain to be between 1 and 4.

5.2 Bandwidth and computation

Even in the absence of faults, REBOUND imposes a cost on the system, by generating and processing heartbeats, and by storing information about modes. To quantify this cost, we initially ran both REBOUND-BASIC and REBOUND-MULTI without a higher-level protocol. We ran simulations for 50 rounds using our synthetic networks and both protocol variants for each topology; we measured, for each node, the storage consumption and the frequency of the cryptographic operations, as well as the bandwidth per link. All measurements were taken in the final round, that is, in steady state.

Figure 5(a) shows our results for bandwidth. REBOUND-BASIC requires a lot of network traffic: its bandwidth consumption grows linearly with the number of nodes, since each node must forward and verify a heartbeat from every other

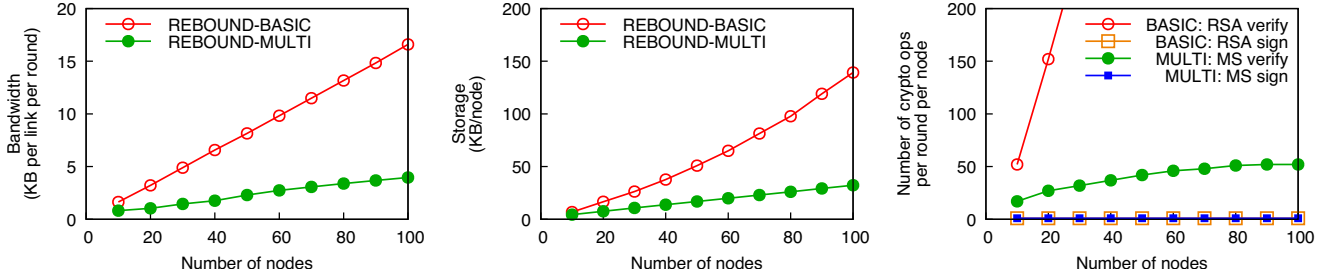


Figure 5. Overhead for the basic REBOUND protocol: (a) bandwidth, (b) storage, and (c) cryptographic operations.

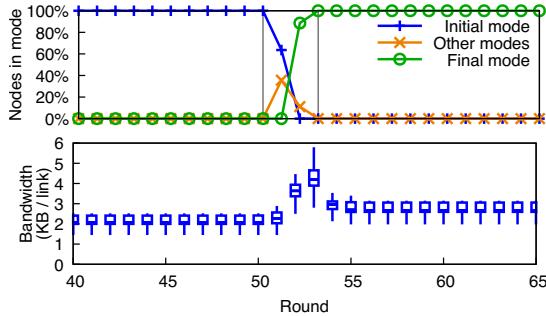


Figure 6. Bandwidth during mode changes: A fault happens in round 50; the change is complete after round 53.

node. In contrast, REBOUND-MULTI’s bandwidth consumption depends mostly on the max-fail distance of the topology, which is roughly the diameter of the graph and thus, for our settings, $O(\ln n)$. At first glance, it may seem that REBOUND’s per-round bandwidth should be even lower because, in stable state, all nodes are in the same mode; however, recall that the multisignatures are aggregated incrementally as heartbeats traverse the network; there is no single point where all the nodes together could sign a given heartbeat for a given round.

Figure 5(b) shows the storage needed for both protocol variants; as before, REBOUND-BASIC handles more heartbeats and thus requires more storage. However, in absolute terms, the storage requirements are fairly small; REBOUND-MULTI requires less than 34 kB for all of the topologies we tried.

Figure 5(c) shows the number of cryptographic operations that a node needs to perform in each round. Both protocol variants generate only one signature per round, but, without multisignatures, REBOUND-BASIC has to verify a lot more of them – its number of verifications grows linearly with both the node degree and the number of nodes in the system. REBOUND-MULTI is clearly more scalable, but its verifications are more expensive; thus, for small topologies (such as our ten-node testbed), it can still be better to use REBOUND-BASIC and its larger number of cheaper verifications.

5.3 Mode changes

When a fault is detected, REBOUND must spread this information throughout the system, and the correct nodes must transition to a new mode. To illustrate this process, we ran a 100-round simulation with REBOUND-MULTI in a 45-node

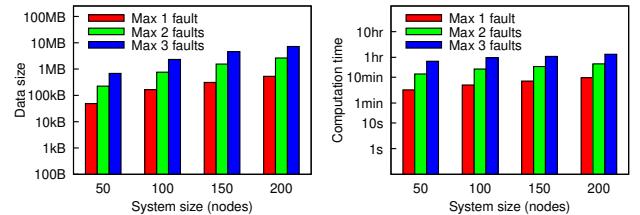


Figure 7. Size of the scheduling trees (a) and time needed to compute them (b).

topology, in which the highest-degree node becomes faulty and performs the most expensive action, which is to declare a different link failure over each of its links (Section 3.6). This initially leads to confusion because different parts of the network transition to different modes at first and take some time to converge on the correct mode.

Figure 6 shows two metrics of interest: the fraction of nodes that is in a given mode (top) and the per-link bandwidth consumption (bottom). When the fault occurs (in round 50), each of the faulty node’s 16 neighbors transitions to a different mode, and, during the following rounds, these modes spread through the system and are partially combined, forming other modes. During this time, the bandwidth consumption briefly increases, partly due to evidence transfers but also due to fewer opportunities for aggregation. However, in round 52, a correct node receives two of the conflicting heartbeats and generates a PoM against the faulty node, which quickly spreads through the rest of the system.

5.4 Scheduling

Once a node transitions to a new mode, it needs to know the set of tasks that it is expected to run. As discussed in Section 3.9, our prototype precomputes schedules for all supported modes and stores them on each node. To evaluate the cost of this computation, we generated schedules for randomized topologies of growing size and workloads, using $f_{\max} = 1 \dots 3$ and $f_{\text{conc}} = 1$. We measured the generation time and the size of the data each node would store.

Figure 7 shows our results. As expected, the size of the tree increases both with the number of nodes n and the maximum number of faults f_{\max} we plan for: the number of vertexes is $\sum_{i=0..f_{\max}} \binom{n}{i}$, one for each set of up to f_{\max} nodes. (f_{conc}

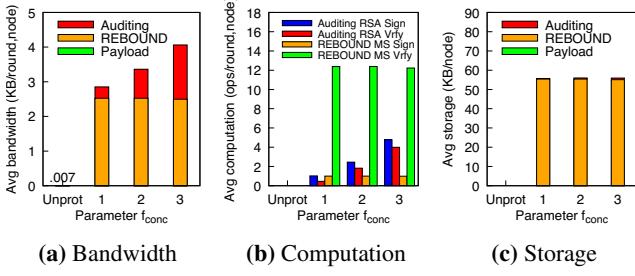


Figure 8. Average per-node runtime costs in the case study.

does not affect the number of vertexes, but it does increase the number of edges.) In absolute terms, the schedules are only a few MB in size, which can easily fit into the available flash memory on many embedded devices. Schedules take between a few minutes and an hour to generate, but this process is entirely offline and is only done once.

5.5 Auditing

Next, we examined the *overall* cost of a BTR deployment, including both REBOUND-MULTI and auditing. We used an example system containing 26 nodes with 4 application flows and ran it for 100 rounds, using the EDF scheduler in our simulator. We looked at two variants: a normal, unprotected system, and one with REBOUND-MULTI and auditing enabled, and configured to protect against $f_{\text{conc}} = 1 \dots 3$ concurrent faults. We measured the number of cryptographic operations, the amount of RAM needed for the protocol (not including the flash memory for the scheduling tree, which was already covered above), and the average per-node network bandwidth.

Figure 8 shows our results. The unprotected system generates fairly little traffic and has no cryptographic operations. Enabling REBOUND adds a fixed overhead, independent of f_{conc} ; in addition, each replica needs to store a copy of the primary’s state, and the primary needs to stream updates to each replica. There is a small $O(f_{\text{conc}}^2)$ term because, when the primary receives a message m , it, and each of its replicas, must relay the m ’s authenticator to the sender’s replicas, but this term is not dominant for small values of f_{conc} .

We note that each replica must also replay the primary’s computation to verify that the primary behaved as expected. This overhead is trivially linear in f_{conc} because each task is effectively executed $f_{\text{conc}} + 1$ times: once by the original node and once by each of the replicas.

5.6 Comparison to BFT

Next, we discuss how REBOUND compares to classical Byzantine fault tolerance (BFT). On comparable hardware, BFT protocols would not be able to run as many applications as REBOUND because they require more replicas – $3f + 1$ in the case of asynchronous protocols, such as the popular PBFT [25], and $2f + 1$ in the case of synchronous protocols, such as [2], which also require fewer rounds. To illustrate this,

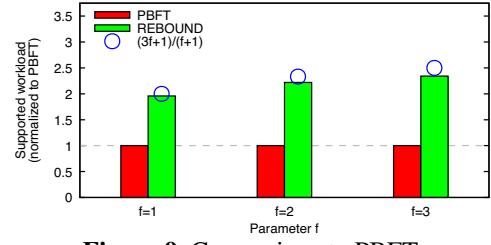


Figure 9. Comparison to PBFT.

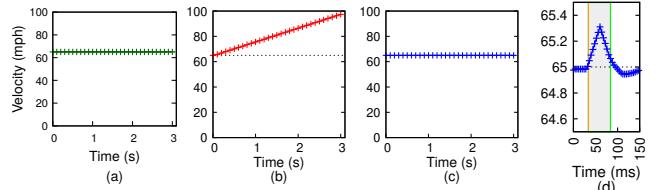


Figure 10. Simulated Volvo XC90 velocity, with cruise control set to 65mph, (a) during normal operation, (b) during an attack, and (c) with REBOUND. (d) shows a detail of (c).

we derived scheduling constraints for PBFT analogous to Section 3.9 (see [51, §F]); then we randomly generated 75 workloads and scheduled them on systems with $N = 25, \dots, 75$ nodes, using either PBFT or REBOUND as a defense. In both cases, we generated more tasks than the systems could handle, and we allowed the schedulers to drop any excess tasks, so the systems were packed with as many tasks as possible. We then measured the median total utilization of the tasks without replicas – that is, how many nodes’ worth of useful work the system can do.

Figure 9 shows our results. The numbers are normalized to the workload that PBFT can support. As expected, REBOUND can, on a given system, run workloads that are at least twice as big as PBFT’s. The ratio closely tracks $\frac{3f+1}{f+1}$ (shown as circles); for large f , it would eventually approach 3. In a comparison to a synchronous BFT protocol, the ratio would approach 2 instead.

5.7 Case study: Volvo XC90

Next, we examine how much damage the adversary can do in a concrete CPS with and without REBOUND. We use a car – specifically, the Volvo XC90 – as a case study; given several widely publicized hacks of cars [30, 48, 49, 80, 99, 119], this seemed like an interesting use case. The XC90 has 38 compute nodes and 13 buses – 1 HCAN, 1 LCAN, 1 MOST, and 10 LIN – for connectivity. The only modification we made was to move the sensors and actuators, which were originally connected directly to specific ECUs, directly onto the CAN buses, so they could also communicate with other ECUs. This change would not be difficult to make in a real car, and it is critical to enabling recovery (otherwise there is a single point of failure).



Figure 11. Behavior of the system from Figure 1 under attack, in an unprotected system (a) and with REBOUND (b-d). Shown are the signals arriving at the valve (yellow), pressure alarm (blue), and monitor (green); the fourth (pink) is the trigger.

Although much about the car is proprietary, we did our best to approximate it – we used the real network topology (Figure 2; taken from [92, §3.5.1]), we chose the timing parameters by benchmarking real automotive controllers (e.g., lane keeping and automated emergency braking) in Simulink [83], and we implemented a few controllers manually, including a PI controller for adaptive cruise control, based on [44, 88] and parameters from the XC90 specifications [117]. More information about our workload is available in [51, §E]. We configure REBOUND for at most $f_{\text{conc}} = 1$ concurrent faults.

Figure 10 shows the simulated vehicle speed for three scenarios; the cruise control is set to 65 mph in each case. In Figure 10(a), the system is working normally, so the speed remains at roughly 65 mph. In the two other scenarios, the adversary compromises the ECM unit (which is responsible for cruise control) and tries to increase the speed as much as possible. This is inspired by real incidents involving sudden unintended acceleration, such as [62]. In Figure 10(b), the system has no defense, so the attack succeeds, and the speed quickly increases to 100mph, within three seconds. In Figure 10(c), REBOUND is enabled, so the system detects the fault and reassigns the cruise-control function to another ECU. Since this happens so quickly – within 50 ms – we also provide a detail in Figure 10(d). The speed rises by only about 0.3 mph; unnoticeable to most drivers.

In this scenario, the “window of opportunity” is provided by the car’s inertia and its limited engine power (235 kW). Although the adversary does briefly have full control over the engine, the impact is limited by the XC90’s maximum acceleration, which is about 4.96 m/s^2 [117].

5.8 Testbed experiments

The experiments so far have been simulations. For our final experiment, we deployed our prototype on our Raspberry Pi testbed (Section 4.1). Recall that there are 10 nodes, and that the topology and workload correspond to Figure 1. We injected three different faults, in which the adversary compromises nodes N4, N3, and N3+N4, respectively; in each scenario, the compromised node(s) start feeding random data to their downstream tasks. This is a worst-case scenario for latency because the fault is discovered only during an audit. We used two configurations, one unprotected and the other configured with $f_{\text{conc}} = 1$ and $f_{\text{max}} = 3$. We measured the

PWM outputs at A_1 (alarm), A_3 (valve), and A_4 (monitor); we omit the signal at A_2 (burner) because we needed one of the oscilloscope’s four channels for the trigger.

Figure 11 shows the actuator outputs in each of the four scenarios; the falling edge on the pink signal at the bottom shows where the first fault was injected. As expected, the unprotected system sends bad data to the actuators indefinitely; in Figure 11(a), this shows up as an irregular pattern on the blue signal. The protected system, on the other hand, quickly recovers and resumes normal operation.

In the first two scenarios – Figures 11(b) and (c) – the adversary is able to disrupt the output of one actuator, whose data flows happens to traverse the compromised node. In each case, the output returns to normal once the system recovers; however, since the system no longer has enough resources to run all four data flows, the least critical flow (to the monitor) is dropped, and the system continues to run without it until the operator can repair and “bless” the compromised node. In the figures, this shows up as a flat green line. Notice that end-to-end recovery takes about 200ms, or five 40ms rounds: if the fault occurs in round r , auditing occurs in round $r + 1$, the evidence is distributed in $r + 2$, the mode transition occurs in $r + 3$, and the new output traverses the data flow in $r + 4$. We could reduce the latency with shorter rounds, at the expense of some additional overhead.

In the third scenario the adversary compromises two nodes; in Figure 11(d), the first fault is indicated by the falling edge on the bottom signal, and the second fault occurs about one second later. Here, the system is forced to drop an additional flow, leaving only the two most critical ones (of which only one is shown in the figures).

6 Related work

Non-adversarial faults: The question of how to build safe, reliable, and fault-tolerant distributed systems has been considered in great detail by several communities, including distributed systems, real-time systems, and control algorithm design. Existing solutions include replication protocols for asynchronous distributed systems like Paxos [77] and Remus [37], fault-tolerant real-time systems like Mars [73] and DeCoRAM [11], fault-tolerant and/or reconfigurable control systems [126], and stream-processing systems like Borealis [12] and Lineage Stash [118]. However, most of this work

has considered various types of “benign” faults, such as hardware defects, software bugs, or electromagnetic interference, whereas we focus on attacks by a malicious adversary.

Byzantine fault tolerance: There is a rich literature on protocols for tolerating Byzantine faults [1, 5, 25, 33, 36, 56, 63, 74, 79, 105, 114, 121, 123], and some of these protocols have been applied to time-critical distributed systems (e.g., in [65, 72, 87]). Many common BFT protocols are asynchronous and thus cannot provide timing guarantees systems, especially under attack [104], although more recent protocols have improved in this respect [8, 34]. There are, however, protocols for partially synchronous systems, such as [86, 124], as well as fully synchronous protocols, such as [2]. BFT++ [84] is explicitly designed for BFT in CPS, but is somewhat constrained because it is designed to also work with legacy systems. The fault-tolerance approach is complementary to BTR: it can fully mask the symptoms of certain attacks, but it requires more replicas and stronger assumptions.

Classical recovery: There is substantial prior work on recovering systems from intrusions when there are no timing constraints. For instance, Warp [26] can retroactively patch security vulnerabilities in database-backed web applications by rolling back the database and replaying inputs using the patched code, and Retro [71] can repair desktop or server machines by selectively undoing the adversary’s changes while preserving legitimate actions. Unlike REBOUND, these systems cannot guarantee time bounds on recovery, but they do reinforce our earlier point that repairing incorrect outputs is often possible, even outside of CPS.

Bounded-time recovery: The idea of systems recovering in bounded time goes back to work on real-time databases [103]. SAUCR [6] observes that most consecutive data center faults are spaced more than 50 ms apart; it switches from a high-performance to high-safety mode when a fault occurs and switches back once recovery occurs. Cascade [50] looks at bounded-time recovery in a broader set of applications that includes CPS, but, like SAUCR, it is limited to crash faults. We had speculated earlier [31] that BTR could be generalized to Byzantine faults but, to our knowledge, REBOUND is the first concrete solution.

Self-stabilization: One way to make a distributed system fault-tolerant is to ensure that it converges to a correct state even if it is started in an incorrect state. This approach was first proposed by Dijkstra [39] and has led to a rich body of work on self-stabilizing systems [4, 20, 22, 41, 42, 54, 55, 66, 69, 76]. Much of the early work assumed that faults are benign and cannot handle malicious nodes that might constantly steer the system away from its goal. Recent work [14, 38, 40, 43, 64, 82] has extended the approach to the Byzantine setting, but this line of work tends to use a very different system model: for instance, it often relies on a global reset mechanism for recovery, it typically does not consider scheduling, deadlines, or task criticality, and it does not provide a time bound for recovery.

Failure detectors: There is an impressive amount of work on fault detection in the context of *failure detectors*, starting from a paper by Chandra and Toueg [28], but this literature conventionally assumes benign crash faults, and usually studies theoretical bounds on the information about failures that is necessary to solve various distributed computing problems [27]. Kahlstrom et al. [70] was the first to focus explicitly on Byzantine faults, but the definitions in [70] are specific to consensus and broadcast protocols. Haeberlen et al. [60] generalized this concept but focused exclusively on the asynchronous setting, without time bounds or support for recovery.

Attack-resistant control: There is an emerging security-oriented research trend within the control and CPS communities (e.g., see [45] and the references therein). However, existing solutions either assume a centralized setting (e.g., [120]) or focus more on attacks on the sensors and actuators, and not on the controllers (e.g., [7, 23, 45, 89, 109]); the latter approach is complementary to ours.

Accountability: Accountability [3, 10, 58–61, 127] provides a way to detect many forms of Byzantine behavior, and it can also generate evidence of detected attacks. However, all of the existing work on accountability assumes an asynchronous system, that is, it cannot detect timing faults, give a bound on the time to detection, or perform recovery.

Multi-mode systems: Many real-time embedded systems can operate in multiple modes that involve different sets of tasks, and transitioning between modes requires elaborate mode-change protocols (MCPs) to prevent deadline misses and other disruptions [47, 96, 98, 102, 107, 112]. Our recovery approach builds on MCPs; however, to our knowledge, all the existing work on MCPs assumes benign faults and cannot work reliably when the system is compromised.

7 Conclusion

We believe that REBOUND can be an interesting new tool in the community’s toolbox for handling Byzantine faults. Although we have demonstrated REBOUND in the context of cyber-physical systems, our approach (and REBOUND itself) is not limited to that domain – it should be applicable to any system that can tolerate bad outputs for a very brief period, such as stream processing or video streaming. As we have shown, there are valuable benefits to be had – including a lower overhead, timing guarantees, a wider range for f_{\max} , and the ability to support gradual degradation.

Acknowledgments

We thank our shepherd, Manos Kapritsos, and the anonymous reviewers for their thoughtful comments and suggestions. This work was supported in part by NSF grants CNS-1563873, CNS-1703936, CNS-1750158, and CNS-1955670, and by ONR N00014-20-1-2744.

References

[1] M. Abd-El-Malek, G. R. Ganger, G. R. Goodson, M. K. Reiter, and J. J. Wylie. Fault-scalable Byzantine fault-tolerant services. In *Proc. SOSP*, 2005.

[2] I. Abraham, D. Malkhi, K. Nayak, L. Ren, and M. Yin. Sync HotStuff: Simple and practical synchronous state machine replication. In *Proc. Oakland*, 2020.

[3] P. Aditya, M. Zhao, Y. Lin, A. Haeberlen, P. Druschel, B. Maggs, and B. Wishon. Reliable client accounting for hybrid content-distribution networks. In *Proc. NSDI*, 2012.

[4] Y. Afek and G. M. Brown. Self-stabilization over unreliable communication media. *Distributed Computing*, 7(1):27–3–4, 1993.

[5] A. S. Aiyer, L. Alvisi, A. Clement, M. Dahlin, J.-P. Martin, and C. Porth. BAR fault tolerance for cooperative services. In *Proc. SOSP*, 2005.

[6] R. Alagappan, A. Ganesan, J. Liu, A. Arpacı-Dusseau, and R. Arpacı-Dusseau. Fault-tolerance, fast and slow: Exploiting failure asynchrony in distributed systems. In *OSDI*, 2018.

[7] S. Amin, A. A. Cárdenas, and S. S. Sastry. Safe and secure networked control systems under denial-of-service attacks. In *Proc. HSCC*, 2009.

[8] Y. Amir, B. Coan, J. Kirsch, and J. Lane. Prime: Byzantine replication under attack. *IEEE Transactions on Dependable and Secure Computing (TDSC)*, 8(4):564–577, 2011.

[9] Z. Anderson and M. Giovanardi. Self-driving vehicle with integrated active suspension, Oct. 2 2014. US Patent App. 14/242,691.

[10] M. Backes, P. Druschel, A. Haeberlen, and D. Unruh. CSAR: a practical and provable technique to make randomized systems accountable. In *Proc. NDSS*, 2009.

[11] J. Balasubramanian, A. Gokhale, A. Dubey, F. Wolf, D. C. Schmidt, C. Lu, and C. Gill. Middleware for resource-aware deployment and configuration of fault-tolerant real-time systems. In *Proc. RTAS*, 2010.

[12] M. Balazinska, H. Balakrishnan, S. R. Madden, and M. Stonebraker. Fault-tolerance in the borealis distributed stream processing system. *ACM Trans. Database Syst.*, 33(1):3:1–3:44, Mar. 2008.

[13] Ben Lynn. PBC Library. Version 0.5.14.

[14] M. Ben-Or, D. Dolev, and E. N. Hoch. Fast self-stabilizing Byzantine tolerant digital clock synchronization. In *Proc. PODC*, 2008.

[15] T. Besselmann and M. Morari. Hybrid Parameter-Varying MPC for Autonomous Vehicle Steering. *European Journal of Control*, 14(5):418 – 431, 2008.

[16] A. Bhat, S. Samii, and R. Rajkumar. Practical task allocation for software fault-tolerance and its implementation in embedded automotive systems. In *Proc. RTAS*, 2017.

[17] A. Boldyreva. Threshold signatures, multisignatures and blind signatures based on the Gap-Diffie-Hellman group signature scheme. In *Proc. PKC*, 2003.

[18] F. Borrelli, A. Bemporad, M. Fodor, and D. Hrovat. An MPC/Hybrid System Approach to Traction Control. *IEEE Transactions on Control Systems Technology*, 14(3):541 – 552, May 2006.

[19] G. Bracha. An asynchronous $\lfloor (n-1)/3 \rfloor$ -resilient consensus protocol. In *Proc. PODC*, 1984.

[20] G. M. Brown, M. G. Gouda, and C.-L. Wu. Token systems that self-stabilize. *IEEE Trans. Comput.*, 38(6):845–852, June 1989.

[21] A. Burns and R. I. Davis. Mixed criticality systems – a review. <http://www-users.cs.york.ac.uk/burns/review.pdf>, Mar. 2019.

[22] J. E. Burns and J. K. Pachl. Uniform self-stabilizing rings. *ACM Transactions on Programming Languages and Systems*, 11(2):330–344, Apr. 1989.

[23] A. A. Cárdenas, S. Amin, and S. Sastry. Research challenges for the security of control systems. In *Proc. HotSec*, 2008.

[24] J. Carrau, A. Liniger, X. Zhang, and J. Lygeros. Efficient Implementation of Randomized MPC for Miniature Race Cars. In *European Control Conference (ECC)*, 2016.

[25] M. Castro and B. Liskov. Practical Byzantine fault tolerance and proactive recovery. *ACM Transactions on Computer Systems*, 20(4):398–461, 2002.

[26] R. Chandra, T. Kim, M. Shah, N. Narula, and N. Zeldovich. Intrusion recovery for database-backed web applications. In *Proc. SOSP*, 2011.

[27] T. D. Chandra, V. Hadzilacos, and S. Toueg. The weakest failure detector for solving consensus. *J. ACM*, 43(4):685–722, July 1996.

[28] T. D. Chandra and S. Toueg. Unreliable failure detectors for reliable distributed systems. *J. ACM*, 43(2):225–267, Mar. 1996.

[29] R. N. Charette. This car runs on code. *IEEE Spectrum*, 2009. <http://spectrum.ieee.org/transportation/systems/this-car-runs-on-code>.

[30] S. Checkoway, D. McCoy, B. Kantor, D. Anderson, H. Shacham, S. Savage, K. Koscher, A. Czeskis, F. Roesner, and T. Kohno. Comprehensive experimental analyses of automotive attack surfaces. In *Proc. USENIX Security*, 2011.

[31] A. Chen, H. Xiao, L. T. X. Phan, and A. Haeberlen. Fault tolerance and the five-second rule. In *Proc. HotOS*, May 2015.

[32] J. Chen, R. Tan, G. Xing, and X. Wang. PTEC: A system for predictive thermal and energy control in data centers. In *Proc. RTSS*, 2014.

[33] B.-G. Chun, P. Maniatis, S. Shenker, and J. Kubiatowicz. Attested append-only memory: Making adversaries stick to their word. In *Proc. SOSP*, 2007.

[34] A. Clement, E. L. Wong, L. Alvisi, M. Dahlin, and M. Marchetti. Making Byzantine fault tolerant systems tolerate Byzantine faults. In *Proc. NSDI*, 2009.

[35] R. P. Collinson. *Introduction to avionics systems*. Springer, 2011.

[36] J. A. Cowling, D. S. Myers, B. Liskov, R. Rodrigues, and L. Shrira. HQ replication: A hybrid quorum protocol for Byzantine fault tolerance. In *Proc. OSDI*, 2006.

[37] B. Cully, G. Lefebvre, D. Meyer, M. Feeley, N. Hutchinson, and A. Warfield. Remus: high availability via asynchronous virtual machine replication. In *Proc. NSDI*, 2008.

[38] A. Daliot and D. Dolev. Self-stabilization of Byzantine protocols. In *Proc. SSS*, 2005.

[39] E. W. Dijkstra. Self-stabilizing systems in spite of distributed control. *Communications of the ACM*, 17(11):643–644, Nov. 1974.

[40] D. Dolev and E. N. Hoch. Byzantine self-stabilizing pulse in a bounded-delay model. In *Proc. SSS*, 2007.

[41] S. Dolev. *Self-Stabilization*. MIT Press, 2000.

[42] S. Dolev, A. Israeli, and S. Moran. Self-stabilization of dynamic systems assuming only read/write atomicity. In *Proc. PODC*, 1990.

[43] S. Dolev and J. L. Welch. Self-stabilizing clock synchronization in the presence of Byzantine faults. *J. ACM*, 51(5):780–799, Sept. 2004.

[44] U. Drolia, Z. Wang, Y. Pant, and R. Mangharam. Autoplug: An automotive test-bed for electronic controller unit testing and verification. In *Proc. ITSC*, 2011.

[45] H. Fawzi, P. Tabuada, and S. Diggavi. Secure estimation and control for cyber-physical systems under adversarial attacks. In *arXiv:1025.5073v1*, 2012.

[46] M. J. Fischer, N. A. Lynch, and M. S. Paterson. Impossibility of distributed consensus with one faulty process. *J. ACM*, 32(2):374–382, Apr. 1985.

[47] G. Fohler. Changing operational modes in the context of pre-runtime scheduling. *IEICE Transactions on Information and Systems*, E76-D(11):1333–1340, 1993.

[48] I. Foster, A. Prudhomme, K. Koscher, and S. Savage. Fast and vulnerable: A story of telematic failures. In *Proc. WOOT*, 2015.

[49] L. Franceschi-Bichhieri. Hacker finds he can remotely kill car engines after breaking into GPS tracking apps, 2019. https://www.vice.com/en_us/article/zmpx4x/hacker-monitor-cars-kill-engine-gps-tracking-apps.

[50] N. Gandhi, E. Roth, R. Gifford, L. T. X. Phan, and A. Haeberlen. Bounded-time recovery for distributed real-time systems. In *Proc. RTAS*, 2020.

[51] N. Gandhi, E. Roth, B. Sandler, A. Haeberlen, and L. T. X. Phan. RE-BOUND: Defending distributed systems against attacks with bounded-time recovery (extended version). Technical Report MS-CIS-21-01, Department of Computer and Information Science, University of Pennsylvania, 2021.

[52] T. Geyer, G. Papafotiou, R. Frasca, and M. Morari. Constrained Optimal Control of the Step-Down DC-DC Converter. *IEEE Transactions on Power Electronics*, 23(5):2454–2464, Sept. 2008.

[53] T. Geyer, G. Papafotiou, and M. Morari. Model Predictive Direct Torque Control - Part I: Concept, Algorithm and Analysis. *IEEE Trans. on Industrial Electronics*, 56(6):1894–1905, June 2009.

[54] M. Gouda and N. Multari. Stabilizing communication protocols. *IEEE Transactions on Computers*, 40(4):448–458, Apr. 1991.

[55] M. G. Gouda, R. R. Howell, and L. E. Rosier. The instability of self-stabilization. *Acta Informatica*, 27(8):697–724, 1990.

[56] R. Guerraoui, N. Knežević, V. Quéma, and M. Vukolić. The next 700 BFT protocols. In *Proc. EuroSys*, 2010.

[57] Gurobi Optimization, Inc. <http://www.gurobi.com>.

[58] A. Haeberlen, P. Aditya, R. Rodrigues, and P. Druschel. Accountable virtual machines. In *Proc. OSDI*, 2010.

[59] A. Haeberlen, I. Avramopoulos, J. Rexford, and P. Druschel. NetReview: Detecting when interdomain routing goes wrong. In *Proc. NSDI*, 2009.

[60] A. Haeberlen and P. Kuznetsov. The Fault Detection Problem. In *Proc. OPODIS*, Dec. 2009.

[61] A. Haeberlen, P. Kuznetsov, and P. Druschel. PeerReview: Practical accountability for distributed systems. In *Proc. SOSP*, 2007.

[62] L. Ham and R. Grace. Cruise control terror for freeway driver. *The Sydney Morning Herald*, Dec. 2009. <https://www.smh.com.au/national/cruise-control-terror-for-freeway-driver-20091215-ktxn.html>.

[63] C. Ho, R. van Renesse, M. Bickford, and D. Dolev. Nysiad: Practical protocol transformation to tolerate Byzantine failures. In *Proc. NSDI*, 2008.

[64] E. N. Hoch, D. Dolev, and A. Daliot. Self-stabilizing Byzantine digital clock synchronization. In *Proc. SSS*, 2006.

[65] K. Hoyme and K. Driscoll. SAFEbus. In *Proc. DASC*, 1992.

[66] A. Israeli and M. Jalfon. Token management schemes and random walks yield self-stabilizing mutual exclusion. In *Proc. PODC*, 1990.

[67] K. Itakura and K. Nakamura. A public key cryptosystem suitable for digital multisignatures. *NEC Research & Development*, 71:1–8, 1983.

[68] K. Jang, J. Sherry, H. Ballani, and T. Moncaster. Silo: Predictable message latency in the cloud. In *Proc. SIGCOMM*, 2015.

[69] S. Katz and K. J. Perry. Self-stabilizing extensions for message-passing systems. *Distributed Computing*, 7(1):17–26, Nov. 1993.

[70] K. P. Kihlstrom, L. E. Moser, and P. M. Melliar-Smith. Byzantine fault detectors for solving consensus. *The Computer Journal*, 46(1):16–35, 2003.

[71] T. Kim, X. Wang, N. Zeldovich, and M. F. Kaashoek. Intrusion recovery using selective re-execution. In *Proc. OSDI*, 2010.

[72] H. Kopetz and G. Bauer. The time-triggered architecture. *Proceedings of the IEEE*, 91(1):112–126, 2003.

[73] H. Kopetz, A. Damm, C. Koza, M. Mulazzani, W. Schwabl, C. Senft, and R. Zainlinger. Distributed fault-tolerant real-time systems: The Mars approach. *IEEE Micro*, 9(1):25–40, 1989.

[74] R. Kotla, L. Alvisi, M. Dahlin, A. Clement, and E. L. Wong. Zyzzyva: Speculative Byzantine fault tolerance. *ACM Transactions on Computer Systems (TOCS)*, 27(4), 2009.

[75] E. Kovacs. Cyberattack on german steel plant caused significant damage. *Security Week*, 2014. <https://www.securityweek.com/cyberattack-german-steel-plant-causes-significant-damage-report>.

[76] H. Kruijer. Self-stabilization (in spite of distributed control) in tree-structured systems. *Information Processing Letters*, 8(2):91–95, 1979.

[77] L. Lamport. The part-time parliament. *ACM Transactions on Computer Systems (TOCS)*, 16(2):133–169, May 1998.

[78] L. Lamport, R. Shostak, and M. Pease. The Byzantine generals problem. *ACM Transactions on Programming Languages and Systems (TOPLAS)*, 4(3):382–401, 1982.

[79] J. Li and D. Mazières. Beyond one-third faulty replicas in Byzantine fault tolerant systems. In *Proc. NSDI*, 2007.

[80] M. Liebowitz. The sound of hacking: Researchers use Trojan CD to hack car. *NBC News*, 2011. http://www.nbcnews.com/id/42074718/ns/technology_and_science-security/t/sound-hacking-researchers-use-trojan-cd-hack-car/#.XYPOBSUpDUY.

[81] F. Maggi. Rogue robots: Testing the limits of an industrial robot's security. TrendLabs, <https://www.dropbox.com/s/7ob04tbhpdjj6ks/tr.pdf>, 2017.

[82] M. R. Malekpour. A Byzantine-fault tolerant self-stabilizing protocol for distributed clock synchronization systems. In *Proc. SSS*, 2006.

[83] MATLAB. *Version 9.7.0 (R2019b)*. The MathWorks Inc., Natick, Massachusetts, 2019.

[84] J. S. Mertoguno, R. Craven, M. Mickelson, and D. Koller. A physics-based strategy for cyber resilience of CPS. In *Defense + Commercial Sensing*, 2019.

[85] S. Micali, K. Ohta, and L. Reyzin. Accountable-subgroup multisignatures. In *Proc. ACM CCS*, 2001.

[86] Z. Milosevic, M. Biely, and A. Schiper. Bounded delay in Byzantine-tolerant state machine replication. In *Proc. SRDS*, 2013.

[87] P. Miner. Analysis of the SPIDER fault-tolerance protocols. In *Proc. NASA Langley Formal Methods Workshop (LFM)*, 2000.

[88] mLAB. Autoplug. <https://github.com/mlab-upenn/AutoPlug/blob/master/Firmware/CruiseControl/Sources/main.c>.

[89] Y. Mo and B. Sinopoli. Secure control against replay attacks. In *Proceedings of the Allerton Conference on Communication, Control, and Computing (ALLERTON)*, 2009.

[90] M. Morari. Fast model predictive control (MPC). Presentation, available from <http://divf.eng.cam.ac.uk/cfes/pub/Main/Presentations/Morari.pdf>.

[91] NIST. Guide to supervisory control and data acquisition (SCADA) and industrial control systems security, 2006. <https://www.dhs.gov/sites/default/files/publications/csd-nist-guidetosupervisoryanddataacquisition-scadaandindustrialcontrolsystemssecurity-2007.pdf>.

[92] T. Nolte. Share-driven scheduling of embedded networks, 2006.

[93] F. Oldewurtel, A. Ulbig, A. Parisio, G. Andersson, and M. Morari. Reducing Peak Electricity Demand in Building Climate Control using Real-Time Pricing and Model Predictive Control. In *Proc. Conference on Decision and Control (CDC)*, 2010.

[94] M. Pajic, J. Weimer, N. Bezzo, O. Sokolsky, G. J. Pappas, and I. Lee. Design and implementation of attack-resilient cyberphysical systems: With a focus on attack-resilient state estimators. *IEEE Control Systems*, 37(2):66–81, April 2017.

[95] G. Papafotiou, J. Kley, K. Papadopoulos, P. Bohren, and M. Morari. Model Predictive Direct Torque Control - Part II: Implementation and Experimental Evaluation. *IEEE Trans. on Industrial Electronics*, 56(6):1906–1915, June 2009.

[96] P. Pedro and A. Burns. Schedulability analysis for mode changes in flexible real-time systems. In *Proc. ECRTS*, 1998.

[97] P. Ramanathan and M. Hamdaoui. A dynamic priority assignment technique for streams with (m, k)-firm deadlines. *IEEE Transactions on Computers*, 44(12):1443–1451, 1995.

[98] J. Real and A. Crespo. Mode change protocols for real-time systems: A survey and a new proposal. *Real-Time Systems*, 26:161–197, 2004.

[99] J. Reindl. Car hacking remains a very real threat as autos become ever more loaded with tech. *USA Today*, 2018. <https://www.usatoday.com/story/money/2018/01/14/car-hacking-remains-very-real-threat-autos-become-ever-more-loaded-tech/1032951001/>.

[100] S. Richter, S. Mariethoz, and M. Morari. High-speed online MPC based on a fast gradient method applied to power converter control.

In *Proc. American Control Conference*, 2010.

[101] E. Roth and A. Haeberlen. Do not overpay for fault tolerance! In *Proc. RTAS*, 2021.

[102] L. Sha, R. Rajkumar, J. Lehoczky, and K. Ramamritham. Mode change protocols for priority-driven preemptive scheduling. *Real-Time Systems*, 1(3):243–264, 1989.

[103] L. C. Shu, J. A. Stankovic, and S. H. Son. Achieving bounded and predictable recovery using real-time logging. In *Proc. RTAS*, 2002.

[104] A. Singh, T. Das, P. Maniatis, P. Druschel, and T. Roscoe. BFT protocols under fire. In *Proc. NSDI*, 2008.

[105] A. Singh, P. Fonseca, P. Kuznetsov, R. Rodrigues, and P. Maniatis. Zeno: Eventually consistent Byzantine-fault tolerance. In *Proc. NSDI*, 2009.

[106] D. Soudbahsh, L. T. X. Phan, A. Annaswamy, O. Sokolsky, and I. Lee. Co-design of control and platform with dropped signals. In *Proc. ICCPS*, Apr. 2013.

[107] N. Stoimenov, S. Perathoner, and L. Thiele. Reliable mode changes in real-time systems with fixed priority or EDF scheduling. In *Proc. DATE*, 2009.

[108] G.-N. Sung, C.-Y. Juan, and C.-C. Wang. Bus guardian design for automobile networking ECU nodes compliant with FlexRay standards. In *Proc. ISCE*, 2008.

[109] A. Teixeira, D. Pérez, H. Sandberg, and K. H. Johansson. Attack models and scenarios for networked control systems. In *Proc. HiCoNS*, 2012.

[110] C. Temple. Avoiding the babbling-idiot failure in a time-triggered communication system. In *Proc. FTCS*, 1998.

[111] D. Tesar. Robot and robot actuator module therefor, Oct. 18 1994. US Patent 5,355,743.

[112] K. Tindell, A. Burns, and A. Wellings. Mode changes in priority preemptively scheduled systems. In *Proc. RTSS*, 1992.

[113] L. Valenta, S. Cohney, A. Liao, J. Fried, S. Bodduluri, and N. Heninger. Factoring as a service. Cryptology ePrint Archive, Report 2015/1000, 2015. <https://eprint.iacr.org/2015/1000>.

[114] B. Vandiver, H. Balakrishnan, B. Liskov, and S. Madden. Tolerating Byzantine faults in transaction processing systems using commit barrier scheduling. In *Proc. SOSP*, 2007.

[115] M. Vasak, M. Baotic, M. Morari, I. Petrovic, and N. Peric. Constrained optimal control of an electronic throttle. *International Journal of Control*, 79(5):465–478, June 2006.

[116] S. Vestal. Preemptive scheduling of multi-criticality systems with varying degrees of execution time assurance. In *Proc. RTSS*, 2007.

[117] Volvo. Xc90 technical data, 2018. Available from <https://www.media.volvocars.com/global/en-gb/models/xc90/2018/specifications>.

[118] S. Wang, J. Liagouris, R. Nishihara, P. Moritz, U. Misra, A. Tumanov, and I. Stoica. Lineage stash: fault tolerance off the critical path. In *Proc. SOSP*, 2019.

[119] G. Warth. New hack: When drivers aren't in control. *San Diego Tribune*, 2015. <https://www.sandiegouniontribune.com/news/education/sdut-ucsd-professor-cyber-hacking-2015aug28-story.html>.

[120] T. Wongpiromsarn, U. Topcu, and R. Murray. Receding horizon temporal logic planning for dynamical systems. In *Proceedings of the 48th IEEE Conference on Decision and Control (CDC)*, 2009.

[121] T. Wood, R. Singh, A. Venkataramani, P. Shenoy, and E. Cecchet. ZZ and the art of practical BFT execution. In *Proc. EuroSys*, 2011.

[122] M. Xu, L. T. X. Phan, H. Y. Choi, and I. Lee. Analysis and implementation of global preemptive fixed-priority scheduling with dynamic cache allocation. In *Proc. RTAS*, 2016.

[123] J. Yin, J.-P. Martin, A. Venkataramani, L. Alvisi, and M. Dahlin. Separating agreement from execution for Byzantine fault tolerant services. In *Proc. SOSP*, 2003.

[124] M. Yin, D. Malkhi, M. K. Reiter, G. G. Gueta, and I. Abraham. HotStuff: BFT consensus with linearity and responsiveness. In *Proc. PODC*, 2019.

[125] M. Yu, L. Wang, T. Chu, and F. Hao. Stabilization of networked control systems with data packet dropout and transmission delays: Continuous-time case. *European Journal of Control*, 11(1):40–49, 2005.

[126] Y. Zhang and J. Jiang. Bibliographical review on reconfigurable fault-tolerant control systems. *Annual reviews in control*, 32(2):229–252, 2008.

[127] W. Zhou, Q. Fei, A. Narayan, A. Haeberlen, B. T. Loo, and M. Sherr. Secure network provenance. In *Proc. SOSP*, 2011.